Radiochimica Acta 72, 169–178 (1996)

On-line Gas Chromatographic Studies of Chlorides of Rutherfordium and Homologs Zr and Hf

By B. Kadkhodayan[2], A. Türler[3], K. E. Gregorich[1], P. A. Baisden[2], K. R. Czerwinski[1], B. Eichler[3], H. W. Gäggeler[3], T. M. Hamilton[1], D. T. Jost[3], C. D. Kacher[1], A. Kovacs[3], S. A. Kreek[1], M. R. Lane[1], M. F. Mohar[1], M. P. Neu[1], N. J. Stoyer[1], E. R. Sylwester[1], D. M. Lee[1], M. J. Nurmia[1], G. T. Seaborg[1], and D. C. Hoffman[1]

[1] **Lawrence Berkeley Laboratory, Berkeley, California, USA**
[2] **G. T. Seaborg Institute for Transactinium Science, Livermore, California, USA**
[3] **Paul Scherrer Institute, CH-5232 Villigen PSI, Switzerland**

(Received June 20, 1995; revised August 29, 1995)

Chromatography / Isothermal / Rutherfordium / Volatility / Adsorption / Enthalpy

Abstract

Gas-phase isothermal chromatography is a method by which volatile compounds of different chemical elements can be separated. The technique, coupled with theoretical modeling of the processes occurring in the chromatography column, provides information about thermodynamic properties (e.g., adsorption enthalpies) for compounds of elements, such as the transactinides, which can only be produced on an atom-at-a-time basis. In addition, the chemical selectivity of the isothermal chromatography technique provides the decontamination from interfering activities necessary for determination of the nuclear decay properties of the isotopes of these elements.

The Zr and Hf isotopes, 30.7-s ^{98}Zr and 38-s ^{162}Hf were produced via the ^{235}U(n,f) and ^{147}Sm(^{20}Ne,5n) reactions, respectively. The 65-s ^{261}Rf was produced via the ^{248}Cm(^{18}O,5n) reaction. A new and more accurate half-life for ^{261}Rf of 78^{+11}_{-6}-s has been measured. Measurements were performed on chloride species of Rf and its group 4 homologs, Zr and Hf and on Zr-bromides using the Heavy Element Volatility Instrument (HEVI). Adsorption enthalpies were calculated for all species using a Monte Carlo code simulation based on a microscopic model for gas thermochromatography in open columns with laminar flow of the carrier gas and the following adsorption enthalpies for the group 4 chlorides were obtained for quartz surfaces: Zr(−74±5 kJ/mol), Hf (−96±5 kJ/mol) and Rf (−77±6 kJ/mol). These results indicate that Rf deviates from the trend expected based on extrapolation of the Zr and Hf values. Further calculations are needed to assess whether this is due to relativistic effects in the transactinide region.

1. Introduction

In the transition region at the end of the actinide series and beginning of the transactinide series, the role of the $7p_{1/2}$ and $6d$ orbitals in the chemistry of these elements is difficult to predict. Early relativistic calculations [1–6] predicted a ground state electron configuration for Lr^0 of [Rn]$5f^{14}7s^27p^1$ instead of [Rn]$5f^{14}6d\,7s^2$ as expected by analogy with Lu^0. Based on extrapolations from this result Keller [3] suggested that the ground state configuration of Rf should be $7s^27p^2$ rather than $6d^27s^2$ analogous to the $5d^26s^2$ configuration of its lighter homolog, Hf. In recent more accurate Multiconfiguration Dirac-Fock (MCDF) calculations, Glebov *et al.* [7] determined that the ground state of Rf should be a J = 2 level consisting mainly (80%) of the $6d\,7s^2\,7p$ configuration with a level only 0.5 eV higher consisting mainly (95%) of the $6d^27s^2$ configuration, while the $7s^27p^2$ state (predicted to be the ground state by Keller) is 2.9 eV above the ground state. Generally, Rf is in a 4^+ oxidation state with an electron configuration of [Rn]$5f^{14}$. The formation of chemical bonds in Rf involves the participation of the empty p and d orbitals which, as discussed above, are close in energy. It is conceivable that Rf compounds may exhibit either p or d element character or possibly a combination of both, due to the hybridization of these empty orbitals. This can possibly lead to very interesting chemical properties not necessarily observed in the lighter homologs (Zr and Hf).

The recent experimental work in the chemistry of transactinide elements has prompted an intense effort in relativistic molecular orbital calculations relevant to the properties of their halides. Various chemical procedures have been devised to investigate the chemical properties of the transactinides. These experiments include solution chemistry using chromatographic and solvent extraction techniques and volatility studies of both the elemental form [8] and of the halides [9–16] using on-line gas chromatographic techniques. Results from gas chromatography measurements are more useful for comparison to relativistic molecular orbital calculations since solvent interactions do not play a part in the chemistry. In a work published in 1990, Zhuikov *et al.* [5] evaluated various experimental approaches for investigating relativistic effects in Rf involving volatilities in the elemental state, thermochromatography of Rf tetrahalides, and the stability of lower oxidation states. It was stated that in gas chromatography experiments (elemental forms) it is hardly possible to distinguish between different possible ground state electronic configurations, as it is extremely difficult to stabilize elements like Hf and Rf in the atomic state at the required high column temperatures of up to

Table 1. Comparison of adsorption enthalpies and entropies from on-line and off-line measurements

Compound	ΔH_{ads} (kJ mole^{-1})[a]		ΔS_{ads} (J mole^{-1} K^{-1})[a]	
	on-line	off-line	on-line	off-line
$NbCl_5$	−69±3	−68± 3	−7±5	−15± 5
$NbOCl_3$	−96±3	−94±13	−31±5	−34±14

[a] Data from [20] Table 1.1.

1500 °C. Thermochromatography of the tetrachlorides or tetrabromides appeared most promising.

Rudolph [17] has investigated the validity of "on-line" gas chromatography measurements of inorganic halides and oxides as a tool in determining adsorption enthalpies and entropies for short-lived nuclides. Adsorption enthalpies and entropies on quartz surfaces were measured, for $NbCl_5$ and $NbOCl_3$, using the 54-s ^{97m}Nb. These results were compared with results from "off-line" gas chromatography measurements. As shown in Table 1, on-line measurements of adsorption enthalpies and entropies were found to provide reliable and reproducible results.

As early as 1966, Zvara *et al.* [12] developed a gas chromatography technique (gas-solid thermochromatography) to separate volatile chlorides of element 104. With this technique, volatile compounds such as $ZrCl_4$ and $HfCl_4$ are separated based on deposition temperature in a quartz chromatography column. This method was used to detect Rf halides, assuming that Rf would form volatile chlorides like its lighter homologs Zr and Hf. After completion of the experiment, fission tracks attributed to an isotope of Rf, were found near the section of the column where Hf was deposited. However, detection by recording fission tracks is insufficient for identifying the atomic number (Z) or mass number (A) of a fissioning species since all information concerning the Z, A and the half-life of the fissioning nucleus is lost.

In 1990, Türler *et al.* [11] studied the volatilities of chlorides and bromides of Hf and Rf using on-line gas chromatography. They detected α-particles from the decay of 78-s ^{261}Rf and its 26-s daughter ^{257}No and registered a number of $\alpha-\alpha$ correlations. This was an unambiguous proof that Rf forms volatile halide species.

The short half-lives and low production rates of the transactinide elements make the study of their nuclear and chemical properties difficult. On-line gas chromatography provides a very fast and efficient chemical separation of transactinides from interfering actinide activities providing an invaluable technique for transactinide studies. Furthermore, chemical properties such as volatility of halide species of the transactinides and homologs can be studied. From these measurements, adsorption enthalpies on various solid surfaces can be calculated, and trends in the periodic table can be investigated. In the current work, we carefully studied the relative volatility of the tetrachlorides of group 4 elements Zr, Hf and Rf.

2. Experimental

Several targets were used in this work for the production of transactinide elements and their lighter homologs. All targets were prepared via a molecular deposition technique [18−20] from an isopropanol solution. This method ensures a thin, adherent, and uniform target.

All irradiations for the production of ^{98}Zr were performed at the PSI **SAPHIR** reactor. A helium-filled beam line provides $(4.6\pm0.5)\times10^6$ thermal neutrons/(s · cm^2) with a beam size of 50 mm in diameter [21]. ^{98}Zr was produced via the neutron-induced fission of ^{235}U. The ^{235}U target with a thickness of 0.180 mg/cm^2, was electrodeposited in a 60-mm diameter on a 4.05 mg/cm^2 aluminum foil.

All irradiations for the production of Hf and Rf isotopes were performed at the LBL 88-Inch Cyclotron. ^{162}Hf was produced by the ^{147}Sm(^{20}Ne^{6+}, 5n) reaction. The 140-MeV (laboratory system) ^{20}Ne^{6+} beam, after passing through the 2.75-mg/cm^2 Be vacuum window, 0.2-mg/cm^2 nitrogen cooling gas and the 2.75-mg/cm^2 Be target backing, was degraded to 122 MeV before striking the target material. The overall thickness of this mixed Sm and Eu target was 0.365-mg/cm^2 (0.214-mg/cm^2 ^{147}Sm, and 0.151-mg/cm^2 ^{nat}Eu). Typical beam currents of 0.1 pμA were used throughout the experiments. The isotopes 41-s ^{162}Hf and 1.7-min ^{165}Hf were produced with cross sections of hundreds of millibarns.

The 78^{+11}_{-6}-s ^{261}Rf (half-life measured in this work, see section 3.2.3) was produced by the ^{248}Cm(^{18}O^{5+}, 5n) reaction with a cross section of 5 nb [22, 23]. The 117-MeV (laboratory system) ^{18}O^{5+} beam from the LBL 88-Inch cyclotron, passing through the same materials as in the previous paragraph, was degraded to 99 MeV before striking the target material. The final thickness of ^{248}Cm in the Cm_2O_3 target material was 0.81-mg/cm^2 (6-mm diameter). Typical beam currents of 0.5 pμA were used throughout the experiments.

All products from nuclear reactions were transported to the gas chromatography system, the Heavy Element Volatility Instrument (HEVI) [24], via a He/MoO_3 gas jet transport system. The recoiling reaction products were stopped in the He and collected on the aerosols in the helium, which continuously swept out the volume behind the target. The activity-laden aerosols were transported by the helium through a 1.6-mm i.d. capillary tube to the gas chromatography apparatus. At LBL all capillaries and tubings used in the transport of the products to HEVI were made of Teflon to eliminate any exchange of oxygen through the capillary walls because the yield of volatile halides was found to be sensitive to oxygen. The total transportation yield of the system ranges from 60−80%.

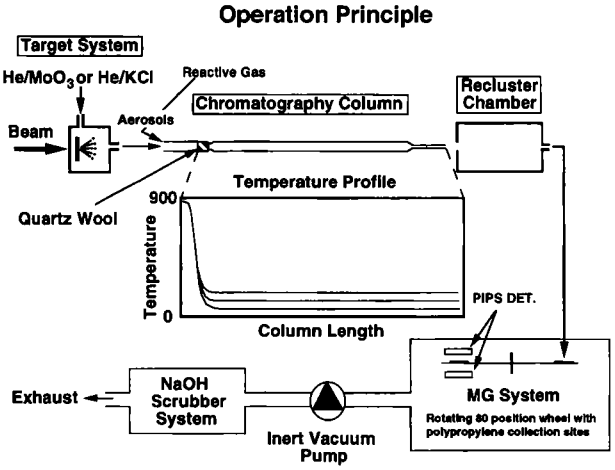

Fig. 1. Illustration of the different parts of the experimental set-up. The experimental process has been followed from production to chromatography and finally to detection.

Potassium chloride aerosols were used in the early development stages of this chemical separation since the He/KCl system was a well-established method of transporting reaction products from heavy ion nuclear reactions. This is the preferred transport system for aqueous chemistry since KCl readily dissolves in aqueous solutions. However, after prolonged gas chemistry experiments with this system, the quartz surface of the chromatography column is partially coated with a thin layer of KCl causing the chromatography to be performed on KCl rather than on SiO_2. Our volatility measurements are strongly dependent on the chromatography surface and therefore a new transport system (He/MoO_3) had to be developed to resolve this problem. Reactions between MoO_3 and a variety of chlorinating agents produce $MoCl_5$ and $MoOCl_3$ which are volatile at temperatures as low as 100 °C. After the transport of reaction products to the chromatography system, the aerosols are converted to volatile species which leave the column without coating the quartz (SiO_2) chromatography surface. The He/MoO_3 transport system is very new and not completely understood. Intensive studies of this system are being conducted at PSI [25].

After transport to HEVI, the activity-laden aerosols enter the first section of the quartz column and are stopped on a quartz wool plug placed at the entrance to the chromatography section of the column (Fig. 1). This first section of the quartz column is kept at approximately 900 °C to vaporize the aerosols, leaving the activity on the quartz wool. Reactive gases are added to the quartz wool plug to form volatile halide compounds which are then carried down a cooler, isothermal section of the column by the helium gas flow.

In isothermal chromatography, the retention times of short-lived activities are measured using their half-lives as a clock. If the half-life is short compared to the retention time, the activity will decay in the column. If the half-life is long in comparison to the retention time, the activity can pass through the column and is available for detection. The species that leave the column enter a recluster chamber, where they are attached to new KCl aerosols in N_2 and are transported to the detection system.

The retention time, and thus the yield of short-lived activities, is dependent on the adsorption enthalpy, the column temperature, the true volume flow rate of the carrier gas and the column length. A Monte Carlo simulation of the processes taking place inside the chromatography column is used to determine ΔH_{ads} by fitting yield as a function of the isothermal column temperature.

All gases were purchased from Matheson Gas Company, Inc. and all other chemicals were purchased from Aldrich Chemical Company, Inc. The HCl gas and the carbon tetrachloride (CCl_4) were 99.995% and 99% in purity, respectively. Experiments were conducted with the halogenating system of HCl gas and a mixture of HCl gas and CCl_4. Further experiments were conducted using a mixture of HCl gas and $SOCl_2$, Cl_2 gas, a mixture of Cl_2 gas and CCl_4, and HBr gas [26]. The quartz chromatography columns provided the SiO_2 surfaces.

In the subsequent of this paper, references will be made to 'direct catch' or 'chemistry' measurements. These are the two types of measurements performed in the gas chemistry experiments. The activity-laden aerosols which exit the target system are either injected into the chromatography system, where chromatography is performed before transport to the detection system for a 'chemistry' measurement, or the chromatography system is bypassed and the activities are sent directly to the detection system where a 'direct catch' measurement is performed. A direct catch is simply a measurement of the amount of activity from specific nuclides under study, without chemical separation. A comparison of the activities from a direct catch measurement and a chemistry measurement gives the relative yield of a species. For experiments conducted at the LBL 88-Inch Cyclotron, the integrated beam current was recorded for each direct catch and chemistry measurement to correct for any beam current fluctuations.

For detection of species with characteristic γ activities (^{98}Zr and ^{162}Hf), a high-purity Ge γ-ray spectrometer system was used in conjunction with a Teflon collection site [26]. During all measurements samples were collected for 5 min and surveyed during the collection period for characteristic photopeaks. All γ-ray spectra (Figs. 2 and 3) from direct catch and chemistry measurements were analyzed using the SAMPO computer code [27]. The output from SAMPO provided energy, total area, total activity, and the respective standard deviations on each value for each peak in the spectrum. In a typical experiment at a certain column temperature, two chemistry measurements were preceded and followed by a direct catch measurement. Corrections were made to peak area values to account for fluctuations in accelerator beam currents and dead time during data collection. Photopeak areas and their

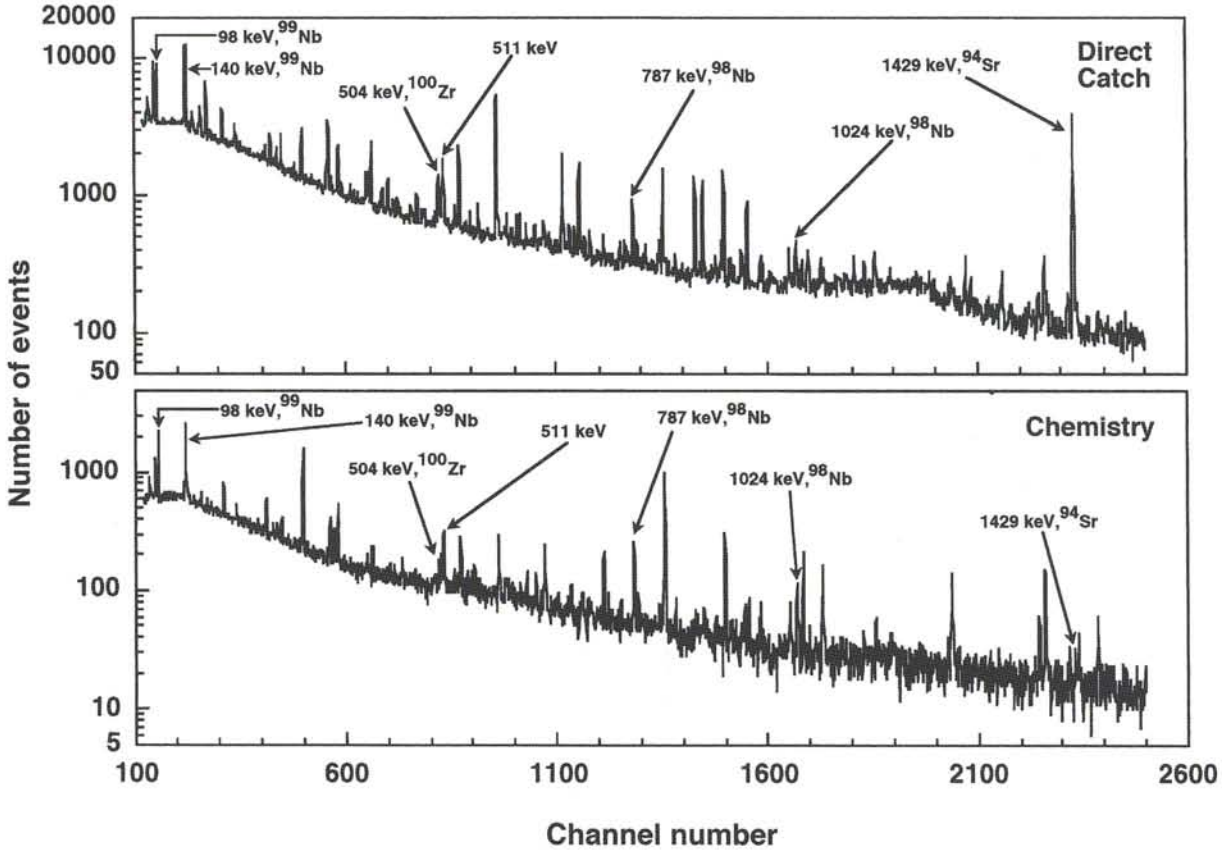

Fig. 2. Typical 5-min γ-spectra of 'direct catch' and 'chemistry' measurements for Zr experiments.

corresponding statistical errors were calculated for the full-energy peaks corresponding to each radionuclide. All peak areas from chemistry measurements conducted at the same temperature were averaged together and the relative yield for each isotope was calculated by a direct comparison of the average areas from the chemistry measurements and the corresponding direct catch measurements.

The Merry-Go-Round (MG) and Realtime Data Acquisition and Graphics System (RAGS) [28, 29] were used for the detection of α/SF activities from the (^{18}O,5n) reaction with ^{248}Cm at the LBL 88-Inch Cyclotron. The 25.4-cm radius horizontal wheel of the MG had 80 equally spaced collection positions about its circumference. A steel ring with a 0.63-cm i.d. hole, which was covered with a 40 ± 10 μg/cm^2 film of polypropylene, was placed in each collection position. The activity-laden aerosols from the gas-jet were deposited on the polypropylene film. The wheel was stepped at one-minute time intervals so as to move the foils consecutively from the collection site into positions between pairs of passivated ion-implanted planar silicon detectors (PIPS). Because of the corrosive nature of the reactive gases used, PIPS detectors were required for this experiment, since they are chemically inert. The MG wheel was replaced with a new one after two complete revolutions in order to minimize the accumulation of any long-lived activities. Six pairs of detectors were used to measure the kinetic energies of coincident fission fragments and alpha particles. The efficiency for detection of α particles in each detector is 30%. Since in this configuration each detection station consists of two detectors, one above and the other below the wheel, the efficiency for the detection of α particles is about 60% and that for coincident fission fragments is about 60%. All events werestored on a hard disk in list mode. Each event was tagged with a time, channel number, and a detector number.

Alpha spectra from all chemistry measurements were analyzed for the number of events in the 8.15–8.38 MeV energy region. This region contains all events due to ^{261}Rf and its 25 ± 2-s daughter ^{257}No (Fig. 4). A weak α line at 8.305 MeV (0.25%) from the 25.2-s ^{211m}Po also falls into this region. For all chemistry measurements the number of events in the 8.15–8.35 MeV range, due to ^{211m}Po, was calculated, based on the intensity of the 7.275-MeV (91.05%) ^{211m}Po alpha line, and subtracted from each spectrum. Corrections were made to account for fluctuations in accelerator beam currents for all measurements. Results from all chemistry measurements conducted at the same temperature were summed together and a plot of relative yield versus temperature was constructed for ^{261}Rf. The same procedure was followed to construct similar plots for ^{211}Bi and ^{211m}Po. The 6.62-MeV and the 7.27-MeV α lines were used for ^{211}Bi and ^{211m}Po, respectively.

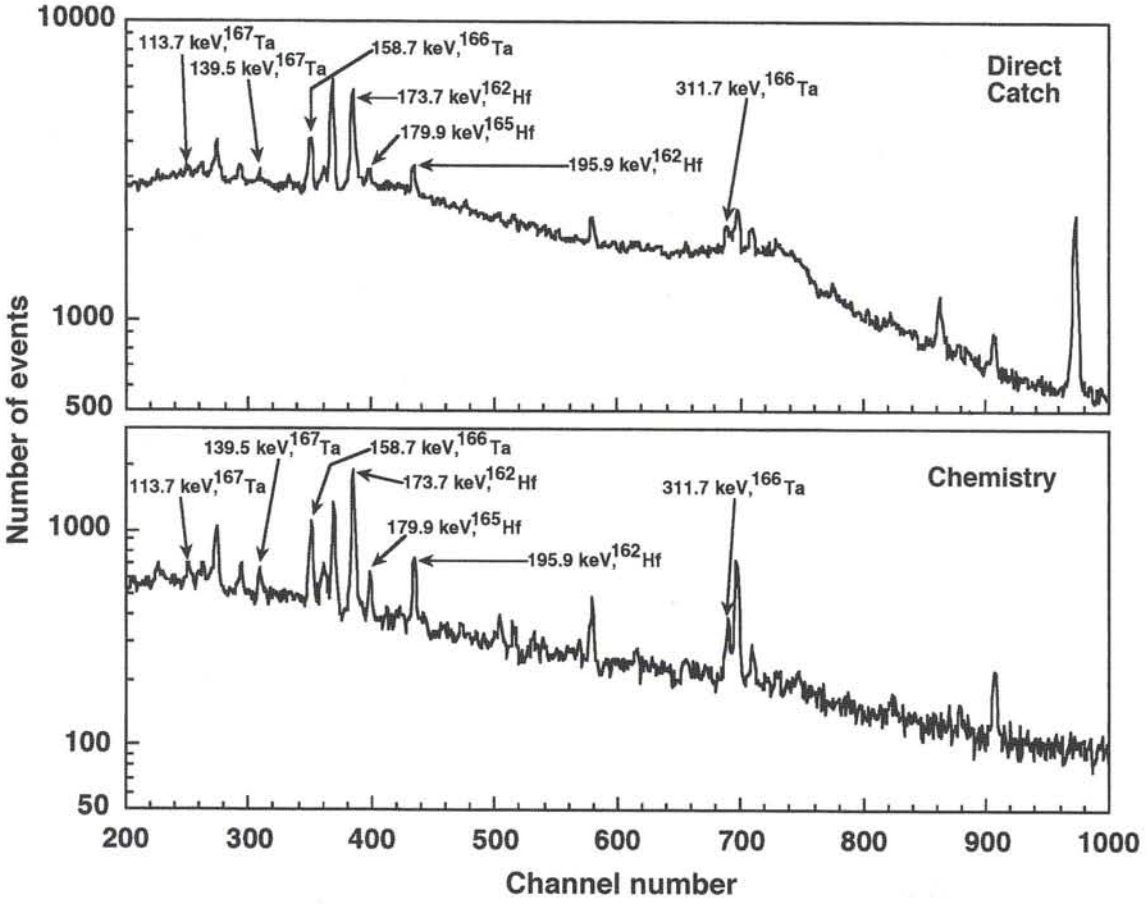

Fig. 3. Typical 5-min γ-spectra of 'direct catch' and 'chemistry' measurements for Hf experiments.

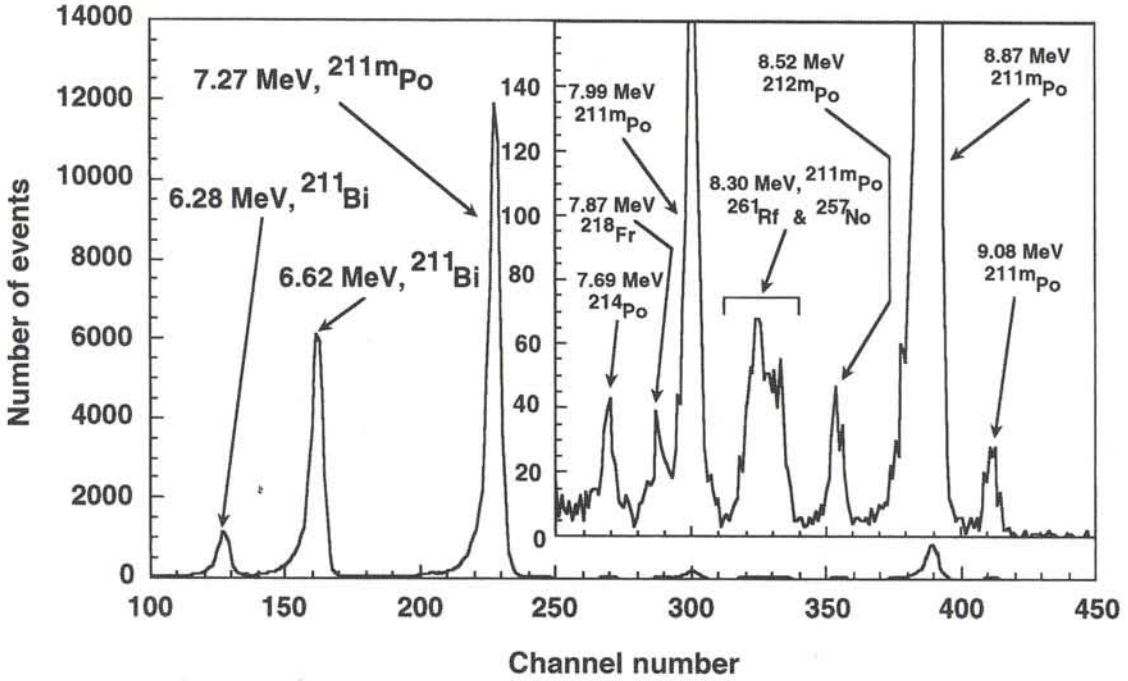

Fig. 4. Sum spectrum of all α particles observed in the Rf chemistry experiments for the first 3 minutes of counting.

To calculate the half-life of ^{261}Rf, all chemistry data were summed together (Fig. 4) and sorted into one-minute intervals. A two-component maximum likelihood [30] decay-curve fit was performed on the 7.275 MeV region of the spectrum. The two components consisted of 25.2-s ^{211m}Po and 3.24-h ^{254}Fm.

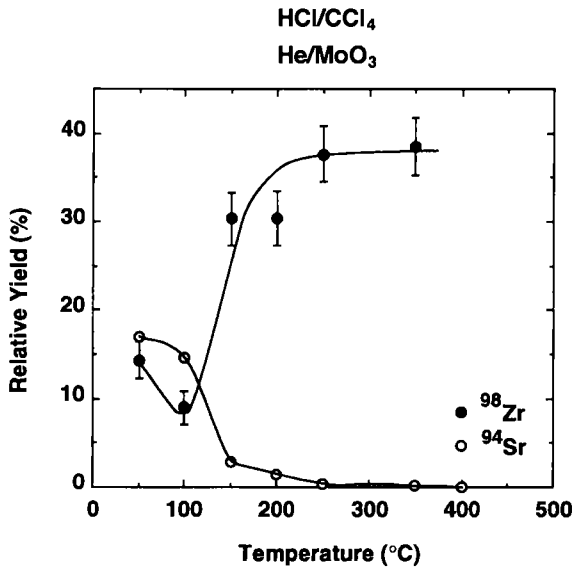

Fig. 5. Relative Yield curves for ^{98}Zr- and ^{94}Sr-chloride molecules with a He/MoO_3 gas jet and HCl/CCl_4 as chlorinating agent.

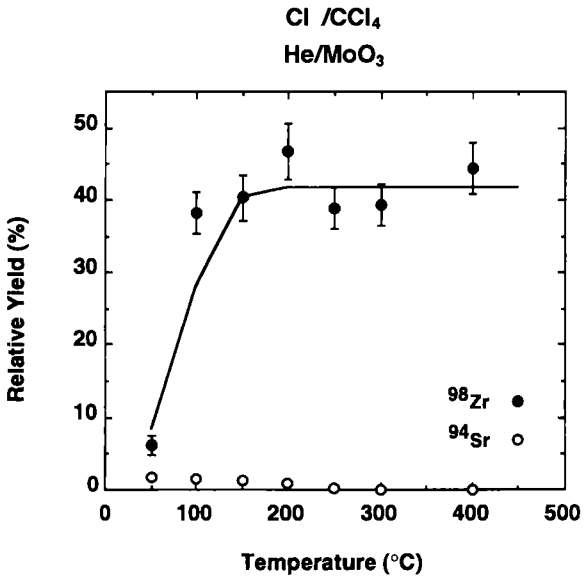

Fig. 6. Relative Yield curves for ^{98}Zr- and ^{94}Sr-chloride molecules with a He/MoO_3 gas jet and Cl_2/CCl_4 as chlorinating agent. The solid line drawn through the data points is from the Monte Carlo computer program.

In this fit half-lives of both radionuclides were fixed. The initial activity for the ^{211m}Po from this fit was used to calculate an initial activity for the 8.305 MeV (0.25%) α line of the same radionuclide. A growth and decay plus one component fit was then performed on the 8.15–8.38 region of the spectrum consisting of ^{261}Rf, its daughter ^{257}No, and ^{211m}Po to arrive at a half-life value for ^{261}Rf. In this fit, half-lives of ^{211m}Po and ^{257}No and the initial activity of ^{211m}Po (calculated from the first fit) were fixed; all other parameters were allowed to vary.

To determine the adsorption enthalpies a Monte Carlo simulation [26] of the yield versus temperature curves has been developed. This Monte Carlo code simulates the processes within the column based on the microscopic thermochromatography model proposed by Zvara [31]. Yield versus temperature plots at given adsorption enthalpy values were generated for each halide molecule. A number of such plots at various adsorption enthalpy values were produced to compare to the experimental data. The adsorption enthalpy value was found by using a weighted least-squares procedure to find the generated plot which best represented the experimental data. The shape of the simulated yield curves matched the experimental data well, confirming the validity of the model proposed by Zvara.

3. Results

Fig. 5 shows a yield curve for $^{98}ZrCl_4$. HCl/CCl_4 was used as the halogenating agent and MoO_3 as transport aerosol. When the halogenating agents containing hydrogen (HCl and HBr) were used, significant yields were unexpectedly oserved at very low temperatures (50 °C to ≈150 °C). During experiments with isotopes of Zr, an isotope of strontium (^{94}Sr) was also produced. Strontium does not form volatile halides. However, significant yields are observed at 50 °C and 100 °C (Fig. 5) for ^{94}Sr. The yield then decreases with increasing temperature to acceptable levels. Therefore, transport by mechanisms other than isothermal chromatography is indicated at very low temperatures when using HBr or HCl as halogenating agents. This complicates the interpretation of the yield curves. When Cl_2/CCl_4 was used as the halogenating agent, the Sr yields at low temperatures were decreased to acceptable levels (Fig. 6), resulting in yield curves which agree well with our Monte Carlo simulations of the isothermal chromatography process.

The results for relative yields are plotted versus temperature. The error bars shown in all yield curves represent one sigma uncertainties based on statistical fluctuations in the peak areas. If no error bars are displayed, the error is smaller than the symbols.

3.1 Bi- and Po-chlorides

Fig. 7 shows a relative yield curve for 2.14-min $^{211}BiCl_3$ and 25.2-s $^{211m}PoCl_4$ with a He/MoO_3 gas-jet and HCl as chlorinating agent. The experimental data (Table 4) were normalized to 100% at maximum yield. As illustrated, the high yield effect at low temperatures is observed at 50 °C for Po. $BiCl_3$ is volatile at 100 °C and $PoCl_4$ is volatile at 150 °C, with respective adsorption enthalpies of −69±4 kJ/mol and −74±5 kJ/mol (Table 2).

The adsorption enthalpy for the Po species agrees well with Rudolph's value of −69±20 [32–33]; however, the Bi value does not. This disagreement may be a result of the large estimated errors in Rudolph's measurements.

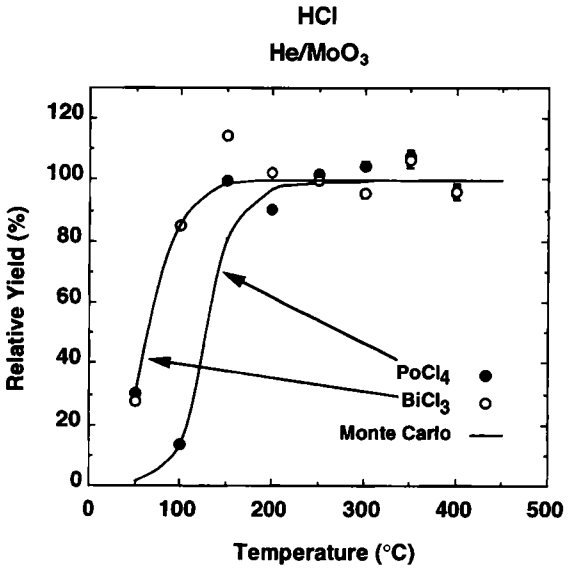

Fig. 7. Relative Yield curves for ^{211}Bi- and ^{211m}Po-chloride molecules with a He/MoO_3 gas jet and HCl as chlorinating agent. The solid lines drawn through the data points are from the Monte Carlo computer program.

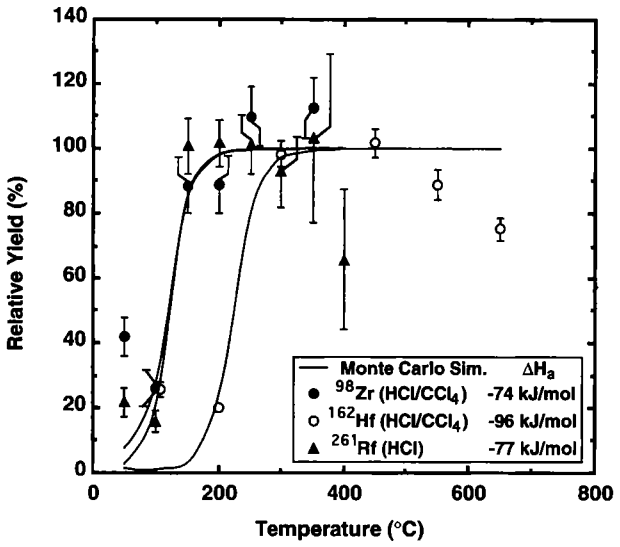

Fig. 8. Relative Yield curves for ^{98}Zr- and ^{162}Hf-, and ^{261}Rf-chloride molecules with a He/MoO_3 gas jet and HCl/CCl_4 as chlorinating agent. The solid lines drawn through the data points are from the Monte Carlo computer program.

3.2 Group 4 elements

3.2.1 Zr-chlorides and -bromides

As depicted in Fig. 8 a sharp increase in relative yield is observed at temperatures between 100 °C and 150 °C for $ZrCl_4$. Table 3 lists the calculated adsorption enthalpies. When KCl was used as the transport aerosol, a decreased volatility on the order of 100 °C was observed for $ZrCl_4$ since the separation was conducted on a partially KCl coated column. This effect is consistent with results of Rudolph [32, 33] for a NaCl surface. As expected, a more negative adsorption enthalpy value was observed. An adsorption enthalpy value of -74 ± 5 kJ/mol for $ZrCl_4$ on a SiO_2 surface is obtained from experiments performed with a He/MoO_3 gas-jet and HCl/CCl_4 as chlorinating agent. Our results show a lower volatility for $ZrBr_4$ in comparison to $ZrCl_4$.

3.2.2 Hf-chlorides

As shown in Fig. 8, a sharp increase in relative yield is observed for $HfCl_4$ at temperatures between 200 °C and 250 °C. Again, when using KCl as transport aerosol material a decrease in volatility (on the order of 150 °C) and adsorption enthalpy is expected. An adsorption enthalpy value of -96 ± 5 kJ/mol for $HfCl_4$ on a SiO_2 surface is obtained (Table 3) from experiments performed with a He/MoO_3 gas-jet and HCl/CCl_4 as chlorinating agent.

3.2.3 Rf-chlorides

A new half life of 78^{+11}_{-6}-s has been measured for ^{261}Rf. This is believed to be a better value than the previous 65 ± 10 s measured by Ghiorso *et al.* [22] because our chemical separation removed a number of contaminants which were present in their spectrum. The resulting correction for ^{211m}Po was much less and, in addition, we performed a multi-component decay analysis. A decay curve is shown in Fig. 9. A total of 1054 α events was observed for ^{261}Rf and its daughter ^{257}No. A total of 170 $\alpha-\alpha$ correlations were observed which corresponds very well to the expected 169 $\alpha-\alpha$ correlations. The expected number of correlations are arrived at considering both true and random correlations of unrelated events. The measured number is inconsistent with expected correlations of random unrelated events. There appears to be a short component in the observed spontaneous fission events. An upper limit of 11% is estimated as the spontaneous fission branch for ^{261}Rf which gives a spontaneous fission half-life of >709 s, assuming no other modes of decay.

A yield curve (Fig. 8) for $^{98}ZrCl_4$, $^{162}HfCl_4$, and $^{261}RfCl_4$ was constructed. Table 4 contains the data

Table 2. Adsorption enthalpies for Bi- and Po-chlorides

Probable compound	Surface	Halogenating agent	Transport aerosol	ΔH°_{ads} (kJ/mol)	ΔH°_{ads} (kJ/mol)[a]
$BiCl_3$	SiO_2	HCl	MoO_3	-69 ± 4	-101 ± 20
$PoCl_4$	SiO_2	HCl	MoO_3	-74 ± 5	-69 ± 20

[a] Data from [32, 33].

Table 3. Adsorption enthalpies for Zr-chlorides and -bromides and Hf-chlorides

Probable compound	Half-life (s)	Surface	Halogenating agent	Transport aerosol	ΔH°_{ads} (kJ/mol)	ΔH°_{ads} [a] (kJ/mol)
$^{98}ZrCl_4$	30.7	SiO_2	Cl_2/CCl_4	MoO_3	−69±6	−97±20
$^{98}ZrCl_4$	30.7	SiO_2	HCl/CCl_4	MoO_3	−74±5	
$^{98}ZrCl_4$	30.7	SiO_2 (KCl)	HCl	KCl	−91±7	−99±20[b]
$^{98}ZrBr_4$	30.7	SiO_2	HBr	MoO_3	−91±6	
$^{162}HfCl_4$	38	SiO_2	HCl/CCl_4	MoO_3	−96±5	
$^{162}HfCl_4$	38	SiO_2	$HCl/SOCl_2$	MoO_3	−101±7	
$^{162}HfCl_4$	38	SiO_2 (KCl)	$HCl/SOCl_2$	KCl	−127±6	−99±20[b]

[a] Data from [32, 33].
[b] Adsorption enthalpy on NaCl surface.

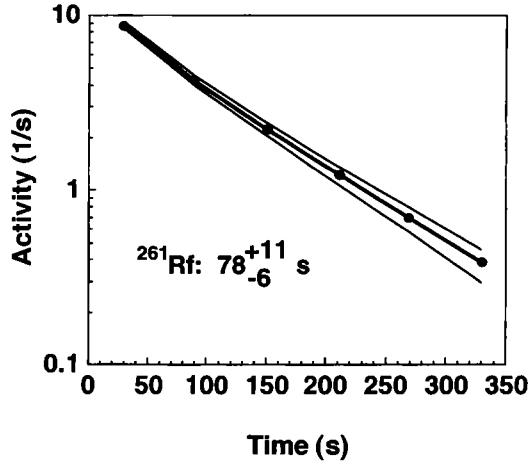

Fig. 9. Growth (^{261}Rf) and decay (^{257}No) plus one component (^{211m}Po) fit to the 8.15 to 8.38 MeV region. In this fit half-lives of Po and No and the initial activity of Po were fixed; all other parameters were allowed to vary. A maximum likelihood decay curve fit has been used. The upper and lower limits on the half-life interval correspond to a confidence level of 68% [30].

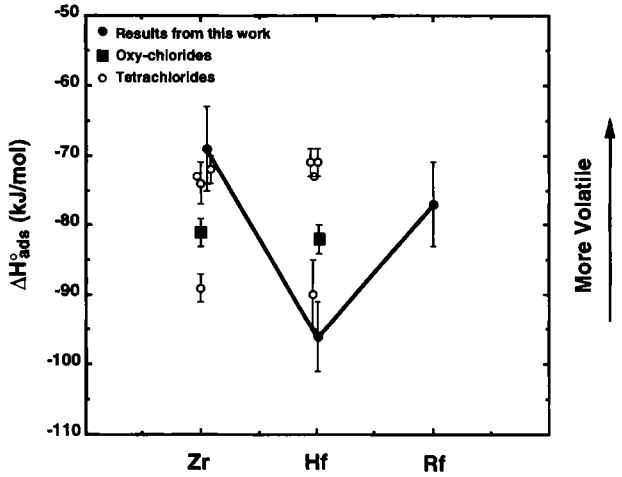

Fig. 10. Adsorption enthalpy values for group 4 chlorides and oxy-chlorides.

used in constructing yield curves for $RfCl_4$. As illustrated, the yield of $RfCl_4$ maximizes at temperatures between 100 °C and 150 °C, corresponding to an adsorption enthalpy value of −77±6 kJ/mol (Table 5).

4. Conclusions

Table 5 gives the adsorption enthalpies (ΔH_{ads}) for chlorides of the group 4 elements on SiO_2 surfaces. As explained earlier, these values result from Monte Carlo simulations based on the yield versus temperature curves and the 50% yield temperatures ($T_{50\%}$) measured in this work. The following adsorption enthalpies were obtained:

$ZrCl_4$ −74±5 kJ/mol

$HfCl_4$ −96±5 kJ/mol

$RfCl_4$ −77±6 kJ/mol.

$HfCl_4$ was found to have a more negative ΔH_{ads} than $ZrCl_4$. Based on a simple extrapolation down the fourth group of the periodic table $RfCl_4$ would be expected to have the most negative ΔH_{ads}, and, therefore, require the highest temperature to reach a maximum yield. The ΔH_{ads} for $RfCl_4$ of −77 kJ/mol deviates from the trend expected from this simple periodic table extrapolation and is similar to that measured for $ZrCl_4$.

In Fig. 10, we have included ΔH_{ads} from other references for Zr- and Hf-tetrachlorides and -oxychlorides. As illustrated, these values vary widely in the literature for both Zr- (−96 to −89 kJ/mol) and Hf-tetrachlorides (−71 to −96 kJ/mol); these variations are far outside the quoted error limits. However, in those experiments where values for Zr and Hf were measured together, their adsorption enthalpies were similar. Our conclusions regarding the deviation from the expected trends in ΔH_{ads} for the group 4 elements were made based only on values from this work, since all elements were studied under same conditions using the same chromatography system (HEVI).

In Ref. [36], the ΔH_{ads} for Zr- and Hf-chlorides were measured as a function of the oxygen concentration. Both Hf and Zr showed two different adsorption enthalpies which were attributed to the tetrachlorides and oxychlorides. The authors found that $ZrOCl_2$ and $HfOCl_2$ had similar adsorption enthalpies which were more negative than the ΔH_{ads} for $ZrCl_4$ and $HfCl_4$

Table 4. Experimental data used in constructing relative yield curves for $BiCl_3$, $PoCl_4$, and $RfCl_4$

Temperature (°C)	Beam integral (pμC)	Total events ^{211m}Po 7.27 MeV	Total events ^{211}Bi 6.62 MeV	Total events ^{261}Rf + ^{257}No + ^{211m}Po 8.18–8.38 MeV	Expected ^{211m}Po events 8.305 MeV	^{261}Rf events 8.18–8.38 MeV
50	10879	2753	1821	40	8	32
100	13656	1516	7045	34	4	30
150	13758	11435	9519	222	31	191
200	18423	13869	11412	296	38	258
250	11813	10010	7142	193	28	165
300	8434	7337	4867	128	20	108
350	2299	2056	1482	39	6	33
400	2263	1803	1315	25	5	20

Table 5. The best volatility and adsorption enthalpy values for all species studied on SiO_2 surface. The temperatures for 50% relative yield are given for comparison, but the complete relative yield versus temperature curve is used in the Monte Carlo calculations to obtain the adsorption enthalpy values

Probable compound	ΔH°_{ads} (kJ/mol)	Temperature (50% yield) (°C)
$BiCl_3$	−69±4	59±5
$PoCl_4$	−74±5	142±5
$ZrCl_4$	−74±5	120±5
$HfCl_4$	−96±5	225±5
$RfCl_4$	−77±6	124±5
$ZrBr_4$	−91±6	198±5

which were also very similar. In addition, for Zr and Hf, the conversion from the pure chloride species to the oxychloride occurred at the same oxygen concentration. It seems that the difference between the ΔH_{ads} measured for Zr and for Hf in our work could be explained by assuming that $ZrCl_4$ and $HfOCl_2$ were measured. However, from the specifics of the experiments, the oxygen concentration for the measurements of the Zr was higher than in the experiments for Hf. Discrepancies between the values of ΔH_{ads} in the literature and our work may be due to slight differences in experimental conditions and the methods by which experimental observables were converted into ΔH_{ads} values. Nevertheless, the deviation in periodic trends observed here is quite interesting and warrants further investigation. More calculations are needed to assess whether or not this is due to relativistic effects in the transactinide region.

The future of on-line gas chromatographic studies in the actinide and transactinide region is both challenging and exciting. The challenging aspect of this research comes from the short half-lives and low production rates of the transactinides. Improvements in detection methods for the existing system (HEVI) should allow studies of elements with half-lives of a few seconds or even less. Presently, volatility studies are being conducted on the bromide systems of group 4 (Zr, Hf, and Rf) and group 5 (Nb, Ta, and Ha) elements. Other elements with available 4^+ oxidation states such as cerium, thorium, plutonium and berkelium will also be investigated.

Acknowledgements

The authors wish to thank the U.S. Department of Energy for the use of the ^{248}Cm, provided through the transplutonium element production facilities at the Oak Ridge National Laboratory. This work was supported in part by the Director, Office of Energy Research, Chemical Sciences Division, U.S. Department of Energy under contract number DE-AC03-76SF00098.

The authors would like to thank the staff and crew of the LBL 88-Inch Cyclotron and the **SAPHIR** reactor at PSI for providing excellent heavy ion beams and neutron beams, respectively.

References

1. Brewer, L.: High Temp. Sci. **17**, 1 (1984).
2. Desclaux, J. P., Fricke, B.: J. Phys. (Paris) **41**, 943 (1980).
3. Keller, Jr., O. L.: Radiochim. Acta **37**, 169 (1984).
4. Pyyko, P.: Chem. Rev. **88**, 563 (1988).
5. Zhuikov, B. L., Glebov, V. A., Nefedov, V. S., Zvara, I.: Int. Conf. Actinides '89, Tashkent, USSR; Radioanal. and Nucl. Chem. Articles **143**, 103 (1990).
6. Brewer, L. J.: Opt. Soc. Am. **61**, 1101 (1971).
7. Glebov, V. A., Kasztura, L., Nefedov, V. S., Zhuikov, B. L.: Radiochim. Acta **46**, 117 (1989).
8. Zhuikov, B. L., Chuburkov, Yu. T., Timokhin, S. N., Jin, K. U., Zvara, I.: Radiochim. Acta **46**, 113 (1989).
9. Gäggeler, H. W., Jost, D. T., Baltensperger, U., Weber, A., Kovacs, A., Vermeulen, D., Türler, A.: Nucl. Instrum. Methods **A309**, 201 (1991).
10. Jost, D. T., Gäggeler, H. W., Vogel, C. H., Schädel, M., Jäger, E., Eichler, B., Gregorich, K. E., Hoffman, D. C.: Inorg. Chim. Acta **146**, 255 (1988).
11. Türler, A., Gäggeler, H., Gregorich, K. E., Barth, H., Brüchle, W., Czerwinski, K. R., Gober, M. K., Hannink, N. J., Henderson, R. A., Hoffman, D. C., Jost, D. T., Kacher, C. D., Kadkhodayan, B., Kovacs, J., Kratz, J. V., Kreek, S. A., Lee, D. M., Leyba, J. D., Nurmia, M. J., Schädel, M., Scherer, U. W., Schimpf, E., Vermeulen, D., Weber, A.,

Zimmermann, H. P., Zvara, I.: J. Radioanal. Nucl. Chem. **160**, 327 (1992).
12. Zvara, I., Chuburkov, Yu. T., Caletka, R., Zvarova, T. S., Shalaevsky, M. R., Shilov, B. V.: Dubna Report D2710 (1966); At. Energ. **21**, 83 (1966); J. Nucl. Energy **21**, 601 (1967); Sov. At. Energy **21**, 709 (1966).
13. Zvara, I., Chuburkov, Yu. T., Caletka, R., Shalaevsky, M. R.: Sov. Radiochem. **11**, 161 (1969).
14. Zvara, I., Chuburkov, Yu. T., Belov, V. Z., Buklanov, G. V., Zakhvataev, B. V., Zvarova, T. S., Maslov, O. D., Caletka, R., Shalaevsky, M. R.: J. Inorg. Nucl. Chem. **32**, 1855 (1970).
15. Zvara, I., Belov, V. Z., Domanov, V. P., Shalaevski, M. R.: Radiokhimiya **18**, 371 (1976).
16. Zvara, I.: Int. Conf. Actinides '89, Tashkent, USSR, September 1989, Abstracts, Nauka, Moscow, p. 989.
17. Rudolph, J., Bächmann, K.: Radiochim. Acta **27**, 105–108 (1980).
18. Aumann, D. C., Müllen, G.: Nucl. Instrum. Methods **115**, 75 (1974).
19. Evans, J. E., Lougheed, R. W., Coops, M. S., Hoff, R. W., Hulet, E. K.: Nucl. Instrum. Methods **102**, 389 (1972).
20. Müllen, G., Aumann, D. C.: Nucl. Instrum. Methods **128**, 425 (1975).
21. Ya Nai-Qi, Jost, D. T., Baltensperger, U., Gäggeler, H. W.: Radiochim. Acta **47**, 1–7 (1989).
22. Ghiorso, A., Nurmia, M., Eskola, D., Eskola, P.: Phys. Lett. **32B**, 95 (1970).
23. Kratz, J. V., Gober, M. K., Zimmermann, H. P., Schädel, M., Brüchle, W., Schimpf, E., Gregorich, K. E., Türler, A., Hannink, N. J., Czerwinski, K. R., Kadkhodayan, B., Lee, D. M., Nurmia, M. J., Hoffman, D. C., Gäggeler, H., Jost, D. T., Kovacs, J., Scherer, U. W., Weber, A.: Phys. Rev. **C45**, 1064 (1992).
24. Kadkhodayan, B., Türler, A., Gregorich, K. E., Nurmia, M. J., Lee, D. M., Hoffman, D. C.: Nucl. Instrum. Methods **A317**, 254–261 (1992).
25. Türler, A.: Private communication.
26. Kadkhodayan, B.: Ph. D. thesis, University of California, Berkeley (1993), Lawrence Berkeley Laboratory Report # 33961, Nuclear Science Division (1993).
27. Routti, J. T., Prussin, S. G.: Nucl. Instrum. Methods **72**, 125 (1969).
28. Hoffman, D. C., Lee, D., Ghiorso, A., Nurmia, M., Aleklett, K.: Phys. Rev. **C22**, 1581 (1980).
29. Leres, R. G.: Lawrence Berkeley Laboratory report # 24808, Engineering Division (1987).
30. Gregorich, K. E.: Nucl. Instrum. Methods **A302**, 135–142 (1991).
31. Zvara, I.: Radiochim. Acta **38**, 95–101 (1985).
32. Rudolph, J., Bächman, K.: J. Chromatogr. **178**, 459–469 (1979).
33. Rudolph, J., Bächman, K.: J. Chromatogr. **187**, 319–329 (1980).
34. Pershina, V., Sepp, W. D., Bastug, T., Fricke, B., Ionova, G. V.: J. Chem. Phys. **97**, 1123 (1992).
35. Pershina, V., Fricke, B.: J. Phys. Chem. **98**, 6468 (1994).
36. Domanov, V. P. *et al.*: Radiokhimiya **31**, 19 (1989).
37. Kim U Zin *et al.*: Isotopenpraxis **24**, 30 (1988).
38. Eichler, B., *et al.*: JINR-Report P12-9454 (1976).
39. Zvara, I., *et al.*: Radiokhimiya **11**, 163 (1969).